JOURNAL OF MATERIALS SCIENCE 27 (1992) 3897–3902

Corrosion behaviour of squeeze-cast aluminium alloy–silicon carbide composites

O. P. MODI, MOHINI SAXENA, B. K. PRASAD, A. H. YEGNESWARAN
Regional Research Laboratory (CSIR), Bhopal 462026 (MP), India
M. L. VAIDYA
Department of Metallurgical Engineering, Indian Institute of Technology, Kanpur 208016 (UP), India

The corrosion behaviour of squeeze-cast Al alloy (LM11) separately dispersed with 10 vol% SiC fibres and SiC particles was investigated in 3% aqueous NaCl solution by general corrosion as well as potentiodynamic polarization techniques. Erosion–corrosion tests were also performed on the specimens in the solution. The base alloy was also subjected to identical tests to examine the influence of the presence of SiC in the matrix. The base alloy showed a lower corrosion rate than the composites. Furthermore, the alloy containing SiC fibres showed a higher corrosion rate than the one with SiC particle dispersion. Erosion–corrosion tests indicated that the rate of material loss followed a trend similar to that in other corrosion tests. The material loss was significantly higher in the case of erosion–corrosion tests. In addition to pitting and attack at the $CuAl_2$ precipitate–Al interface in the matrix, dispersoid–matrix interfacial attack by the corrosion medium was also observed in the case of composites. On the other hand, erosion–corrosion revealed occasional partial removal of the dispersoid due to the impingement of the electrolyte. The tendency of the dispersoid removal by the impinging electrolyte was predominantly more in the case of the composites dispersed with SiC fibres. Results are explained in terms of the interfacial bonding as well as the shape of the dispersoid.

1. Introduction

Al–SiC composites are emerging as potential materials for a variety of engineering applications such as pistons in the automotive industry as well as components such as track shoes, wheels and speed brakes in tanks and aircraft because of their high strength-to-weight ratio and good wear resistance characteristics [1–4]. In recent years considerable interest has been shown in using these composites in marine applications [5]. This requires the examination of the corrosion properties of the composites under identical environments to assess their performance for such applications. The erosion–corrosion properties of the composites become equally important in view of tidal motion of the environment leading to premature failure of components.

It has been observed that 2024 Al alloy dispersed with 20 vol % SiC showed a 40% higher corrosion rate than the base alloy in 3% aqueous NaCl solution [6]. Pitting was found to initiate at the dispersoid–matrix interface [6]. Another investigation related to polarization studies on 2024 Al–20 vol % SiC composite in 0.1 M NaCl indicated a lower pitting potential of the composite than for the matrix alloy [7]. Corrosion studies of Al dispersed with SiC in various forms (particulates, whiskers and continuous fibres) have also been carried out in tidal sea-water immersion. Corrosion pits in this case were found to concentrate around SiC particulates, suggesting that crevices formed at the matrix–dispersoid interface [8].

In view of the possible applications of Al alloy–SiC composites in marine structures such as agitators, impellers and those involving the pumping of fluids [9], the corrosion behaviour of these composites in 3% NaCl solution under normal immersion as well as erosive–corrosive conditions was studied in the present investigation. The base alloy was also subjected to identical tests to observe the effects of SiC in the matrix.

2. Experimental procedure

2.1. Composite preparation

Al–4.5Cu–0.12Fe (LM11) was used as the matrix alloy for the preparation of the composites. Composites consisting of random distributions of 10 vol % each of silicon carbide (SiC) particles (size 15–30 μm) and SiC fibres (length 3 mm and diameter 10–15 μm) were produced by the squeeze-casting technique [10]. In brief, the process involves dispersion of dispersoid in the melt followed by squeeze-casting in a die of appropriate size.

0022–2461

2.2. Corrosion studies

The corrosion behaviour of the alloy and composites was investigated in 3% NaCl solution in atmospheric conditions using techniques such as general corrosion (normal immersion), erosion–corrosion and potentiodynamic polarization. All of the test specimens were metallographically polished according to standard metallographic procedures before being subjected to corrosion tests.

2.3. General corrosion

Specimens in the form of discs (diameter 15 mm and thickness 6 mm) with a hole at the periphery were suspended in a glass container containing 3% NaCl solution. Specimens after the tests were taken out at different time intervals, cleaned, dried and weighed in a Mettler microbalance. Corrosion rates were determined by weight loss measurements.

2.4. Potentiodynamic polarization

Potentiodynamic polarization studies were carried out using a microprocessor-based EG & G Princeton Applied Research (PAR) electrochemical measurement system. The polarization measurements were obtained at a scan rate of 1 $mV\,s^{-1}$ with reference to a saturated calomel electrode (SCE). Each specimen was allowed to reach a stable corrosion potential before starting the polarization scanning.

2.5. Erosion–corrosion

Erosion–corrosion studies were performed using the rotating-sample test method [11]. In this test disc-type specimens (diameter 15 mm and thickness 6 mm) were attached at the periphery of an acrylic disc at a radius of 4 cm and mounted axially on a non-conducting spindle. The disc assembly containing the specimens was rotated about its axis in a tank made of acrylic sheet in 3% NaCl solution with the help of an electric motor to give a linear speed of 1.25 $m\,s^{-1}$. Samples after each cycle were cleaned, dried and weighed. A cycle in this case consisted of normal dipping of the specimens for 18 h in 3% NaCl followed by subjecting them to a rotational speed corresponding to the above linear velocity for 6 h in the same solution.

2.6. Metallography

Specimens were metallographically polished and etched with Keller's reagent for microstructural observations by scanning electron microscopy (SEM). Corroded surfaces as well as their transverse sections were also examined by SEM. The transverse sections were cold-mounted in polyester resin, metallographically polished and etched with Keller's reagent. Before SEM examinations the specimens were sputtered with gold.

3. Results and discussion

Fig. 1a and b shows the microstructure of LM11–SiC

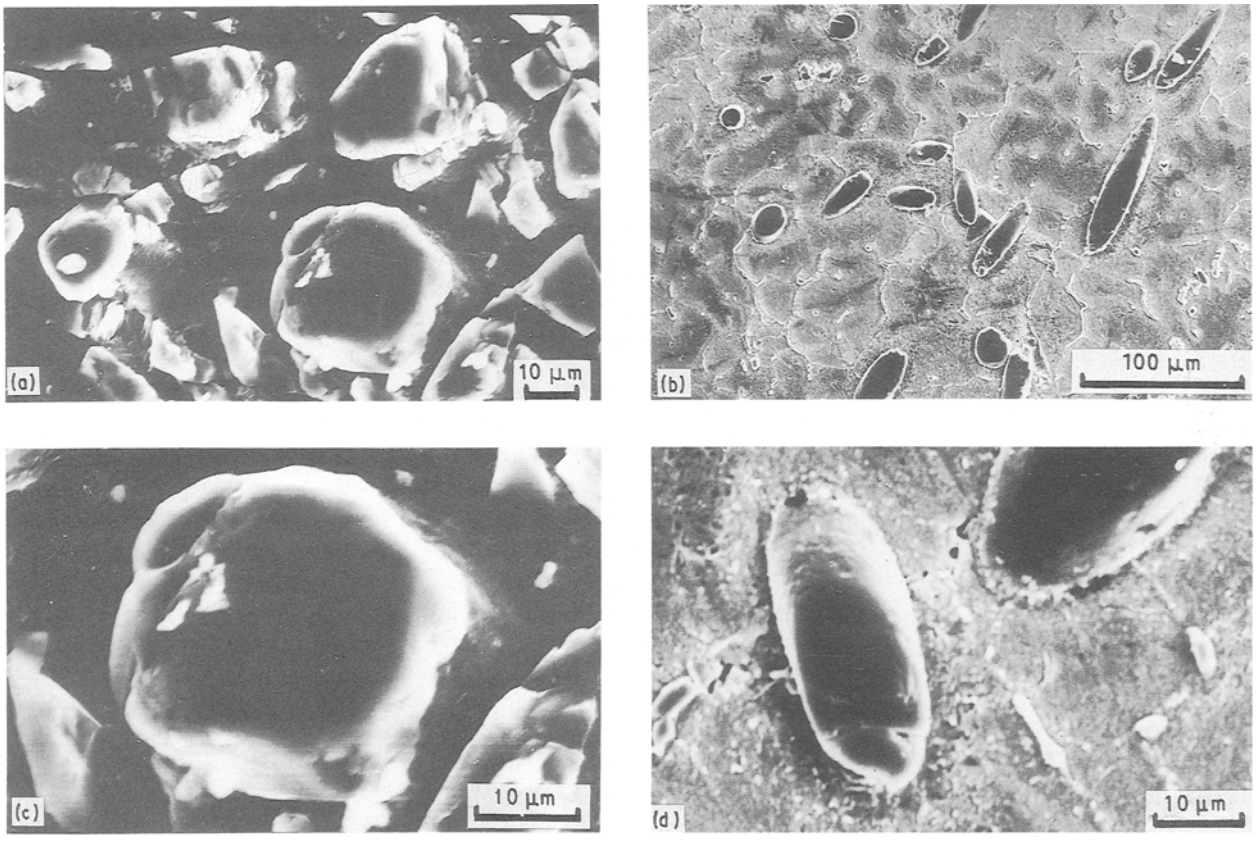

Figure 1 SEM micrographs of metallographically polished surfaces of LM11 alloy dispersed with (a and c) SiC particles and (b and d) SiC fibres, showing (d) interfacial porosity in the case of the SiC fibre composite and (c) good bonding at the dispersoid–matrix interface in LM11–SiC particle composite.

particle and LM11–SiC fibre composites, respectively, revealing the uniform distribution of the dispersoid phase. Good dispersoid–matrix interfacial bonding in the case of the LM11–SiC particle composite (Fig. 1c) and interfacial porosity at the fibre–matrix interface (Fig. 1d) were also observed.

Fig. 2 shows the general corrosion behaviour of the base alloy and composites containing SiC in 3% NaCl. It is seen from the figure that the base alloy showed the least weight loss, while the composite dispersed with SiC fibres showed the most material loss. The Al alloy–SiC particle composite showed a weight loss intermediate between the two in the solution studied. The material loss of the base alloy as well as composites was found to increase with increasing duration of exposure (Fig. 2). Initially the loss was low up to a certain duration, e.g. 8 and 4 days of exposure in the case of the base alloy and the composites, respectively. The rapid rise in material loss after the specified duration of exposure was due to the incubation period required for the breaking of the oxide layer by chloride ions [12]. The shorter incubation period observed in the case of composites could be attributed to the large number of interfaces due to the presence of dispersoid which, in turn, facilitated the formation of pits. Fig. 3 shows the corrosion rate (computed from Fig. 2) of the Al alloy and composites as a function of exposure time. The reduction in the rate of material loss (Fig. 3) could be attributed to the retarding action of the corrosion process by the accumulation of reaction products such as $Al(OH)_3$ on the specimen surface [13]. Such products are formed when the solution inside the corrosion pits is saturated with aluminium cations. This lowers the pH of the solution in the pit, leading to the formation of corrosion products [13].

Fig. 4 shows the weight loss of the base alloy and composites with test duration resulting from the erosion–corrosion test. The weight loss of the base alloy as well as that of the composites increased with the test duration. The trend in this case was similar to

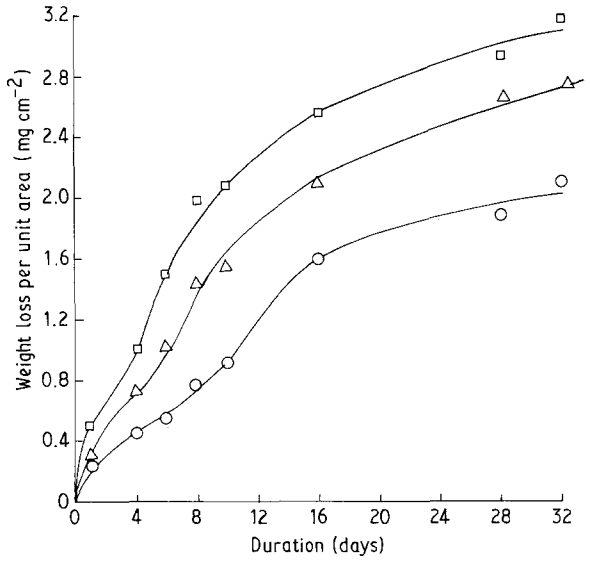

Figure 2 Weight loss as a function of time of exposure in 3% NaCl solution in the general corrosion test: (○) LM11, (△) LM11–SiC particles and (□) LM11–SiC fibres.

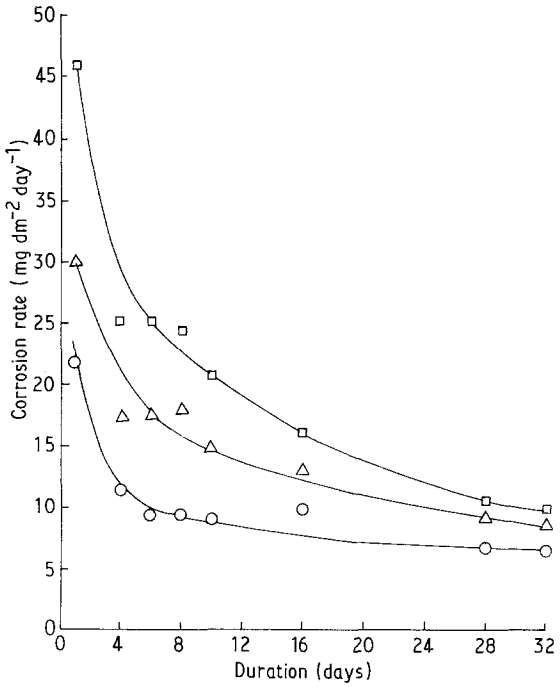

Figure 3 Corrosion rate versus time of exposure in 3% NaCl solution in the case of the general corrosion test: (○) LM11, (△) LM11–SiC particles and (□) LM11–SiC fibres.

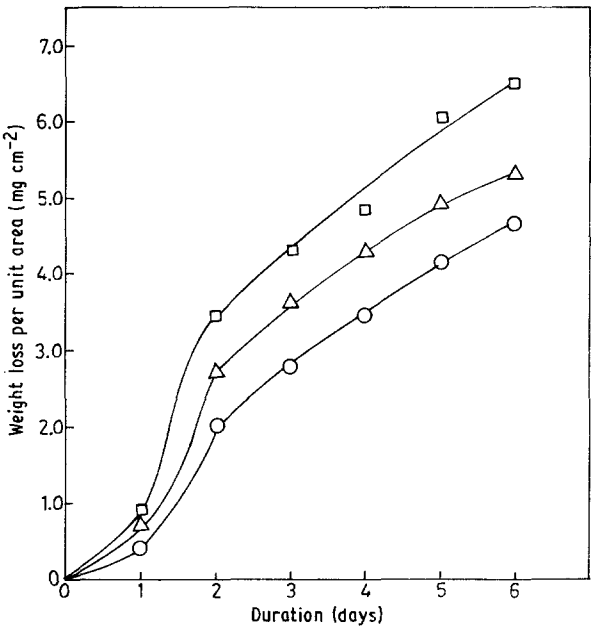

Figure 4 Weight loss versus time of exposure in the case of the erosion–corrosion test: (○) LM11, (△) LM11–SiC particles and (□) LM11–SiC fibres.

that observed in general corrosion (Fig. 2). The incubation period was also reduced to 1 day in all cases (Fig. 4), which was significantly less than that in the case of general corrosion (8 and 4 days for the alloy and composites, respectively; Fig. 2). The increase in material loss in the erosion–corrosion test was found to be 5–10 times higher than the corresponding weight loss obtained in the general corrosion test. This was due to continuous removal of the corrosion product by the impingement of the electrolyte in the former case.

The erosion–corrosion rate of the base alloy and composites with the time of exposure is shown in Fig. 5. The rate was found to be maximum after 2 days of exposure in all cases. Four stages of the erosion–corrosion rate, namely an incubation period (stage I), accelerated erosion (stage II), deceleration period (stage III) and a steady-state condition (stage IV) [14], can be seen in the figure. During erosion the metal surface develops a uniform undulation, leading to the nucleation of smooth-edged pits. These pits then grow into crater-like depressions the material of whose lips is removed by ductile fracture [14]. Corrosive environments accelerate erosion by oxidation, hydroxide formation and formation of micropits by hydrogen evolution resulting in the weakening of the metal [14]. The peak in Fig. 5 corresponds to the appearance of the first deep crater leading to faster rate of material removal [15]. However, entrapment of gas bubbles in the crater reduces the extent of direct contact of the medium with the metal surface, thereby suppressing the erosion rate [15], corresponding to stage III of the Figure. The steady-state erosion–corrosion rate (stage IV) could be a result of the counterbalancing effects of factors such as the formation of deeper craters leading to increased material removal and the entrapment of air in the craters causing a reduction in the weight loss.

Fig. 6 shows the potentiodynamic polarization curves of the alloy and the composites. The corrosion potential of LM11 alloy, LM11–SiC particle and LM11–SiC fibre composites measured after 10 min immersion in 3% NaCl solution were -668.82, -656.17 and -640.53 mV, respectively. This shows a marginal shift in the corrosion potential of the base alloy due to the presence of SiC and is attributed to the non-conducting nature of the SiC [5]. However,

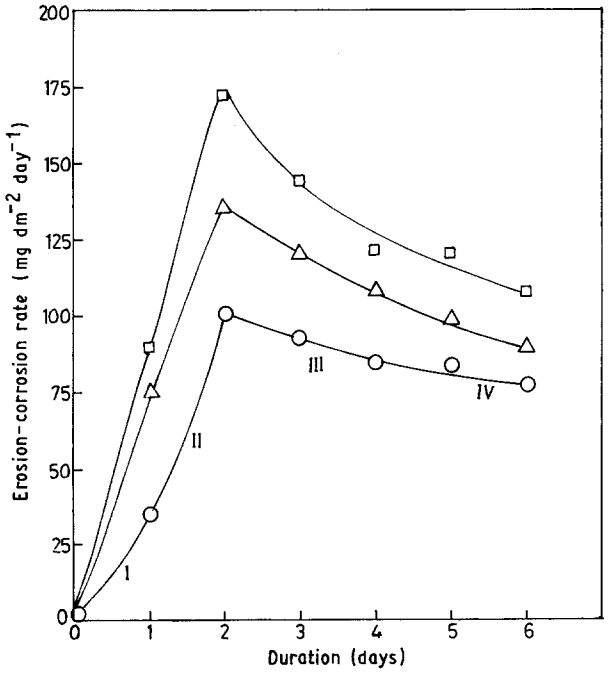

Figure 5 Erosion–corrosion rate versus time of exposure, showing four stages of erosion–corrosion, namely: I, incubation period; II, acceleration; III, deceleration; and IV, steady state: (○) LM11, (△) LM11–SiC particles and (□) LM11–SiC fibres.

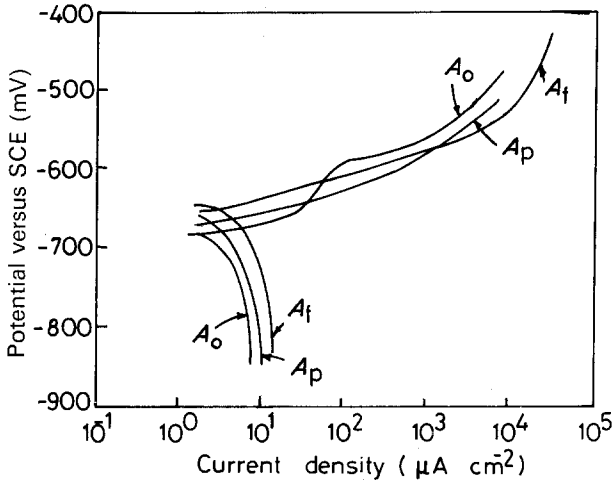

Figure 6 Potentiodynamic polarization curves in 3% NaCl solution. A_o, Base alloy; A_p, alloy containing SiC particles; and A_f, alloy dispersed with SiC fibre.

the corrosion current density for the base alloy dispersed with SiC fibres was found to be higher (7.96 μA cm^{-2}) than that of the one containing SiC particles (4.73 μA cm^{-2}) and the base alloy (3.0 μA cm^{-2}). Furthermore, no sharp pitting potential could be observed for the composites, whereas one of -600 mV was noted in case of the base alloy. This was attributed to a greater passivation tendency of the base alloy than that of the composites.

Fig. 7a to d shows the corroded surfaces of the base alloy and composites after the erosion–corrosion test. The interdendritic corrosion around the $CuAl_2$ precipitate of the base alloy can be seen in Fig. 7a. This was due to the cathodic nature of the latter to the α-Al, which provides a continuous corrosion path along the precipitate [16]. Fig. 7a also shows a lower number of pits of larger size. On the other hand, the composite revealed relatively large number of pits of smaller size (Fig. 7b and c). Fig. 7d shows a typical example of protrusion of the dispersoid from the matrix as a result of preferential matrix removal by the corrosive medium. This was due to the availability of a large interfacial area (owing to the presence of the dispersoid–matrix interface in addition to $CuAl_2$ precipitate) on which corrosion pits could easily nucleate. Fig. 7e is a SEM micrograph of a transverse section of the corroded surface, which reveals the interfacial attack by the electrolyte. The silicon carbide–matrix interface has been suggested to be a more-preferred site for the breakdown of the passive film and the formation of pits [5]. This explains the greater extent of attack on the composite over the base alloy by the electrolyte. With increasing time the electrolyte penetrated deeper at the interface and the matrix preferentially corroded around the dispersoid. This caused protrusion of the reinforcement (Fig. 7b to d). The protruded phase detached itself from the matrix and fell off when not in a position to be adequately supported by the matrix (Fig. 7b). This explains the higher rate of material loss of the composites than the base alloy. The higher l/d ratio, sharp tips and edges as well as poor dispersoid matrix interface (Fig. 1d) further enhanced the extent of attack by the electrolyte

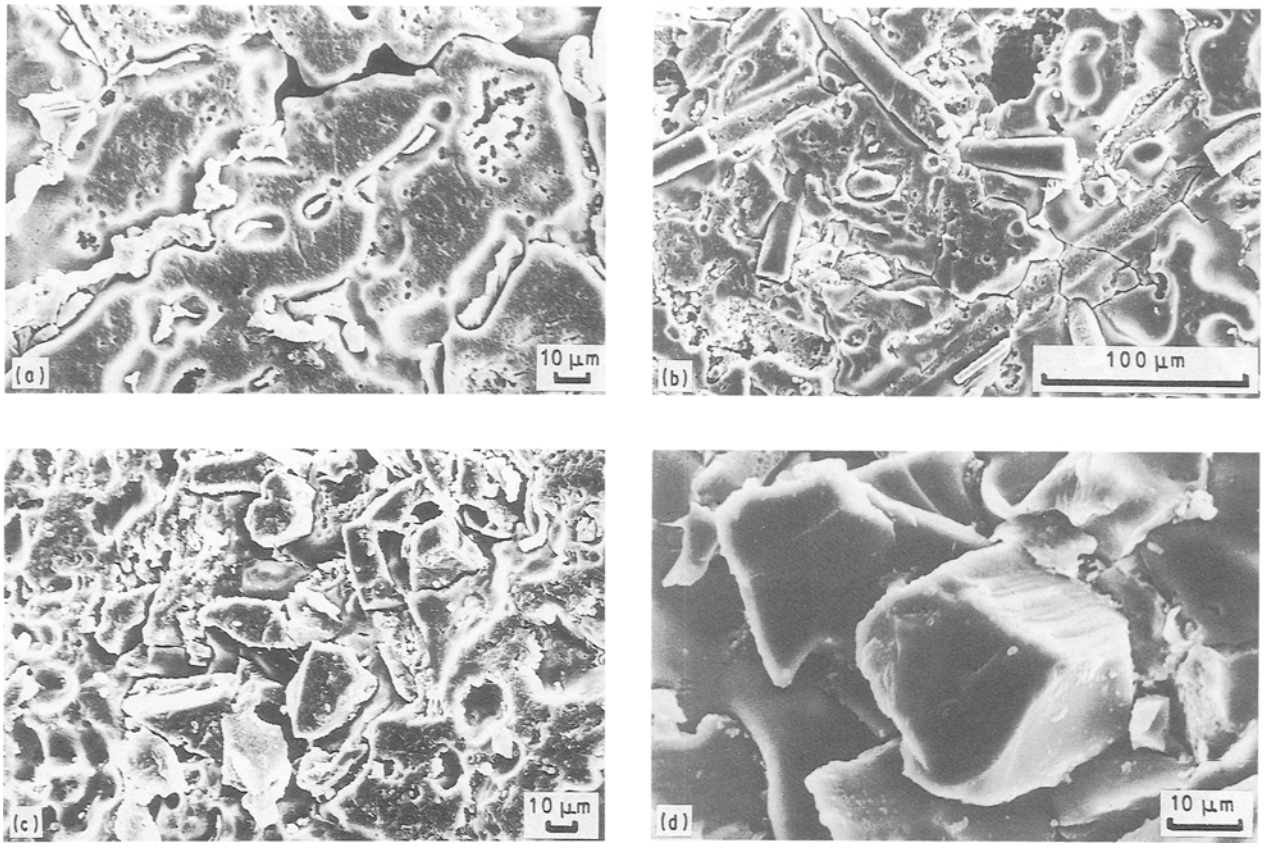

Figure 7 SEM of (a) the base alloy, (b) the alloy containing SiC fibres and (c and d) the alloy reinforced with SiC particle after the erosion–corrosion test. Dispersoid–matrix and $CuAl_2$–Al interfacial attack by the corrosive medium were the common features. Partial removal of the fibres (b) and protrusion of the particles in the matrix (c and d) may also be noted. A typical transverse section of the particle composite (e) shows the clear-cut formation of pits at the dispersoid–matrix interface.

and the removal of the dispersoid, ultimately leading to a higher rate of material removal. These events were more predominant in the case of fibre composite than for particle composite, leading to a higher rate of material loss of the former. It is observed that in the case of composite containing SiC particles the dispersoid–matrix interface was good and the edges of the dispersoid were smoother.

4. Conclusions

The composite containing SiC fibres suffered from the highest rate of material removal and the base alloy showed the lowest rate in general corrosion as well as erosion–corrosion tests. The weight loss was 5–10 times higher in the erosion–corrosion tests under the conditions investigated. This was due to the greater tendency of the protruded dispersoid phase as well as other corrosion products towards removal from the specimen surface by the impinging action of the electrolyte.

The presence of the dispersoid–matrix interface was found to play a dominant role in enhancing the rate of material loss of the composites. Moreover, the poor interface as well as the sharp tips and higher aspect ratio of the dispersoid of SiC fibre composite increased the material loss further.

Addition of SiC in LM11 alloy did not show any significant change in its corrosion potential, whereas an appreciable change was noticed in the corrosion current density of the same, indicating the non-conducting nature of the dispersoid and higher rate of material removal of the composites.

The reinforcement of SiC in LM11 alloy increased the susceptibility of pitting at the dispersoid–matrix interface. A higher number of smaller pits due to the larger interfacial area available for easy nucleation of the pits was observed in the case of the composites, whereas the base alloy showed a smaller number of large pits.

Acknowledgements

The authors are grateful to the Director, RRL, Bhopal, for granting permission to publish this paper. Thanks are also due to Professor A. A. Das, Loughborough University of Technology, UK, for supplying the material.

References

1. I. F. RICHARDSON, *Foundrymen* **82** (1989) 538.
2. K. J. BHANSALI and R. MEHRABIAN, *J. Metals* **32** (1982) 30.
3. F. RANA and D. M. STEFANESCU, *Met. Trans.* **A20** (1989) 1564.
4. A. T. ALPAS and J. D. EMBURY, *Scripta Metall.* **24** (1990) 931.
5. D. M. AYLOR and P. J. MORAN, *J. Electrochem. Soc.* **132** (1985) 1271.
6. D. M. AYLOR, in "Metals handbook", 9th Edn, Vol. 13 (American Society for Metals International, Metals Park, Ohio, 1987) p. 859.
7. E. McCAFFERTY and P. P. TRZASKOMA, in Extended Abstracts of the Electrochemical Society, Denver, Colorado, Meeting, October 1981 (Electrochemical Society, Pennington, New Jersey, 1981) Abstr. 152.
8. D. M. AYLOR and R. M. KAIN, "Recent advances in composites in the United States and Japan", ASTM STP 684, edited by J. R. Vinson and M. Taya (American Society for Testing and Materials, Philadelphia, Pennsylvania, 1985) p. 632.
9. J. ZAHAVI and H. J. WAGNER, in Proceedings of the Symposium on the Corrosion–Erosion Behaviour of Materials, edited by K. Natesan, Fall Meeting of the Metals Society of AIME, St Louis, Missouri, 17–18 October 1978 (American Institute of Mining, Metallurgical and Petroleum Engineers, Warrendale, Pennsylvania, 1978) p. 226.
10. A. A. DAS, M. YACOUB, B. ZANTOUT and A. J. CLEGG, *Cast Met.* **1** (1988) 69.
11. B. VYAS, in "Erosion–Corrosion Treatise on Materials Science and Technology", Vol. 16: "Erosion", edited by C. M. Preece (Academic Press, New York, 1979) p. 364.
12. H. H. STREHBLOW, in International Congress on Metallic Corrosion, June 1984 (National Research Council, Canada, 1984) p. 99.
13. C. EDELEANU and U. R. EVANS, *Trans. Faraday Soc.* **47** (1951) 1121.
14. B. VYAS and C. M. PREECE, in "Erosion, wear and interfaces with corrosion", ASTM STP 567 (American Society for Testing and Materials, Philadelphia, Pennsylvania, 1974) p. 77.
15. J. W. TICHLER, *J. Lubr. Technol. Trans. Amer. Soc. Mech. Engs* **92** (1970) 220.
16. M. METZGER and S. G. FISHMAN, *Indust. Eng. Chem. Prod. Res. Dev.* **22** (1983) 294.

Received 4 April
and accepted 30 July 1991